ELSEVIER

Thermochimica Acta 324 (1998) 165–174

thermochimica acta

Characterising the glass transition and relaxation kinetics by conventional and temperature-modulated differential scanning calorimetry

John M. Hutchinson*

University of Aberdeen, Fraser Noble Building, Department of Engineering, King's College, Aberdeen AB24 3UE, Scotland, UK

Abstract

Over the past 20 years or so, considerable research effort has been directed towards a better understanding of the glass transition in polymers (indeed, of amorphous materials in general), and of the associated relaxation processes, principally by the use of differential scanning calorimetry (DSC). The extent to which phenomenological approaches (e.g. 'curve fitting' and 'peak shift') can describe the response of glasses in DSC is reviewed, and the degree of enlightenment afforded by these models is discussed. More recently, the technique of temperature-modulated DSC (TMDSC), has attracted considerable attention, and its application to the glass transition of polymers is considered here within the framework of the same models as are used for conventional DSC. In particular, the two techniques of DSC and TMDSC are compared in respect of the quantitative analysis of the data and in the light of the problems of heat transfer.

Keywords: Differential scanning calorimetry (DSC); Glasses; Glass transition; Polymers; Temperature-modulated DSC

1. Introduction

Careful and extensive experimental work over many decades has identified a number of aspects of the glass transition and of the glassy state which may be considered to be universally accepted. These would include, for example, the kinetic character of the glass transition, the non-equilibrium nature of the glassy state, and the complex relaxation behaviour that can result from these. A consequence of the latter is that the structure and associated properties (mechanical, optical, physical, electrical, etc.) of glasses can be influenced profoundly by the thermo-mechanical history of the glass formation. It is, therefore, of interest from a fundamental point of view, as well as being of practical importance in many instances, to be able to model the structural changes that occur in glasses during relaxation. One approach is to identify the structure through the measurement of a bulk property such as the enthalpy (by differential scanning calorimetry (DSC)) or the specific volume (by dilatometry), the former method being by far the most common nowadays. By comparing the experimentally observed enthalpic response with the predictions of a theoretical model, it is hoped that some insight may be gained into the glass transformation process. This phenomenological approach has been rather widely used over the past 20 years or so, with results that require careful scrutiny. Such scrutiny of the DSC data is attempted in the present paper, as is an assessment of the possible contribution of temperature-modulated DSC (TMDSC) to this debate.

2. Phenomenological models

Current phenomenological models for structural relaxation are based on two well-accepted and key

*Corresponding author. Tel.: +44-1224-272791; fax: +44-1224-272497; e-mail: j.m.hutchinson@eng.abdn.ac.uk

0040-6031/98/$ – see front matter
PII: S0040-6031(98)00532-2

features, namely 'non-linearity' and 'non-exponentiality'. Non-linearity describes the dependence of the relaxation time(s) on both the temperature (T) and the structure of the glass, and is often written in the form:

$$\tau = A \exp\left[-\theta(T - T_g)\right] \exp\left[-(1-x)\theta\delta_H/\Delta C_p\right] \quad (1)$$

where A is a pre-exponential parameter equal to the relaxation time in equilibrium at the glass-transition temperature T_g, θ a parameter describing the temperature dependence of τ and is related to the apparent activation energy $\Delta h^*(\theta \approx \Delta h^*/RT_g^2)$, and x $(0 \leq x \leq 1)$ the Narayanaswamy parameter [1] which introduces the non-linearity. The structure of the glass is defined here by δ_H, the excess enthalpy, and ΔC_p is the increment in specific heat capacity at T_g. An alternative representation is in terms of the fictive temperature T_f [2]:

$$\tau = A \exp\left[x\Delta h^*/RT + (1-x)\Delta h^*/RT_f\right] \quad (2)$$

These formalisms are often referred to as the Tool–Narayanaswamy–Moynihan (TNM) model [1–3].

The non-exponentiality may be introduced in one of two ways: either as a discrete distribution, as in the KAHR model [4], or more usually by means of the stretched exponential response function:

$$\Psi = \exp\left[-(t/\tau)^{\beta}\right] \quad (3)$$

where exponent $\beta(0 \leq \beta \leq 1)$ is inversely related to the width of the distribution of relaxation times.

These two features, together with a constitutive equation expressing the rate of relaxation as being directly proportional to the departure from equilibrium, are sufficient to describe the response of a glass to any prescribed thermal history. The most common thermal histories employed are isothermal recovery, following a quench from equilibrium, and, in the case of DSC, a three-step cycle involving cooling from equilibrium at a rate q_1, isothermal annealing at a temperature T_a for a period of time during which the enthalpy reduces by an amount $\bar{\delta}_H$, and then reheating through the transition region at a rate q_2. A schematic illustration of the three-step thermal cycle is shown in Fig. 1. The last step is the one that gives rise to an enthalpy overshoot, resulting in the typical endothermic peak seen in the DSC response which is widely used for the evaluation of the key parameters characterising the relaxation kinetics (x, Δh^* and β). The

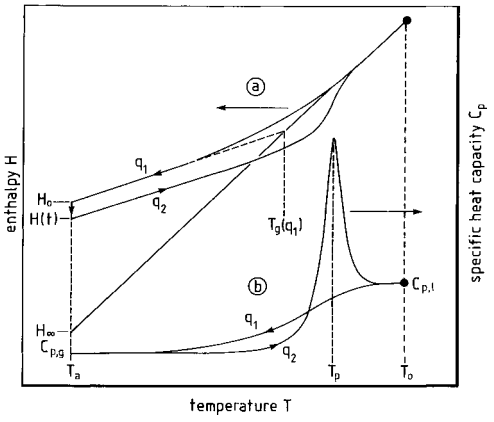

Fig. 1. Schematic illustrations of the isobaric variation of (a) enthalpy H and (b) specific heat capacity C_p with temperature T during a typical three-step thermal cycle. The start and finish of the cycle are indicated by the solid circles. The enthalpy loss during annealing at T_a is $\bar{\delta}_H = H_0 - H(t)$.

two commonly used approaches for the evaluation of these parameters are the 'curve-fitting' and 'peak-shift' methods.

The curve-fitting method [5] fits the predictions of the theoretical model to typical DSC endothermic traces, such as that shown in Fig. 1(b), by a simultaneous adjustment of the three aforementioned parameters together with the pre-exponential parameter A. Ideally, all such DSC curves should be able to be fitted with the same set of parameter values; in practice, this is not usually the case and, instead, some variations are seen with, for example, increasing annealing time (see the discussion in a review by O'Reilly [6]). The peak-shift method [7], on the other hand, examines specifically the dependence of the peak endotherm temperature on the experimental parameters (q_1, $\bar{\delta}_H$ and q_2). Illustrations of each of these dependences are shown in Figs. 2–4, respectively, where the endothermic peak temperature shifts can be seen clearly. For each of these shifts, in the limiting condition of well-stabilised glasses, a direct evaluation of x may be made independently of the other parameters [7]. In this case, the activation energy and the non-exponentiality parameter may be found from further independent experiments [3,8]. Both the approaches suffer from some limitations: in the curve-fitting method, for example, the need to account for thermal gradients in the sample may be critical, whereas in the peak-shift method the attainment of strictly limiting conditions is difficult to

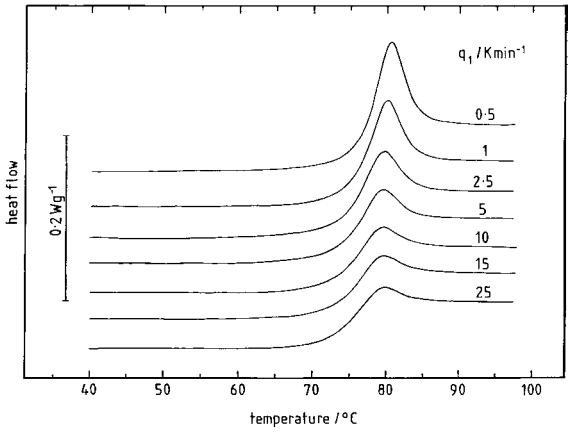

Fig. 2. DSC scans on polypropylene isophthalate illustrating the shift of the peak endotherm temperature with cooling rate (q_1), indicated against each curve. The experimental conditions were: zero annealing at lower temperature T_a=50°C; heating rate q_2=10°C/min. (Redrawn from Ref. [13] with permission.)

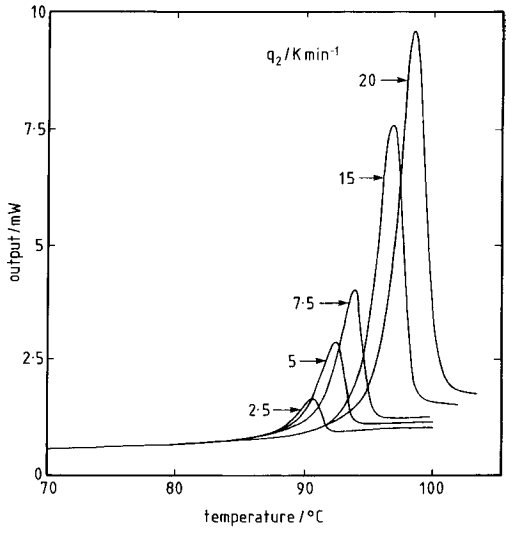

Fig. 4. DSC scans on silver iodomolybdate glass ($AgI–Ag_2O–M_0O_3$ with 40% AgI) illustrating the shift of the peak endotherm temperature with heating rate (q_2), indicated against each curve. The experimental conditions were: cooling rate q_1=20°C/min; and annealing time 96 h at T_a=65°C. (Reproduced from Ref. [17] with permission.)

ensure. Probably for these reasons, as well as others, the parameter values are not always consistent, and any interpretation of their significance must be made with appropriate caution.

An extensive list of values found mainly by the curve-fitting method is given in the review by Hodge [5], whereas a list of values found by the peak-shift method is given in Table 1, taken from Hutchinson [9]. Despite the problems of lack of consistency

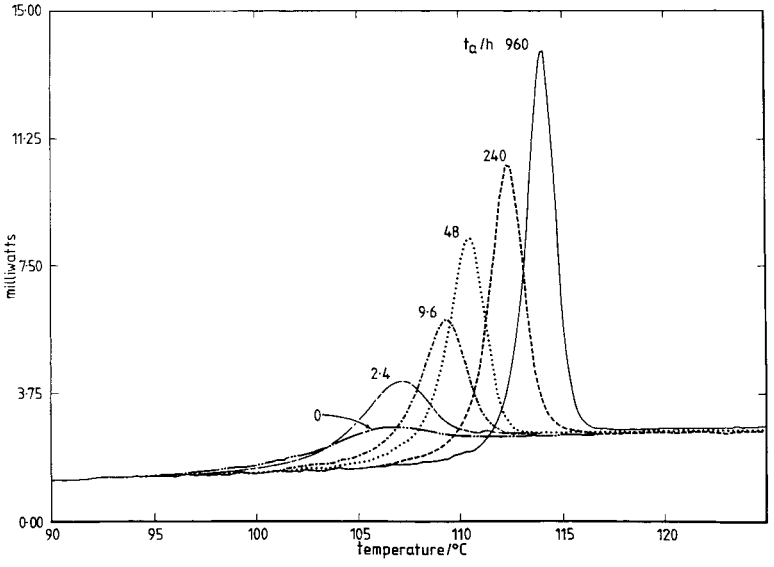

Fig. 3. DSC scans on polystyrene illustrating the shift of the peak endotherm temperature with annealing time (and hence with enthalpy loss $\bar{\delta}_H$), indicated against each curve. The experimental conditions were: cooling rate q_1=20°C/min; annealing temperature T_a=85°C; and heating rate q_2=10°C/min.

Table 1
Values of the relaxation parameters x, β and Δh^* (kJ/mol) found by the peak-shift method. The values of Δh^* and $\beta\Delta h^*$ have been rounded to 0 or 5; the values of $x\Delta h^*$ use the original unrounded values of Δh^*

Glass	x	β	Δh^*	$\beta\Delta h^*$	$x\Delta h^*$	Ref.
PVC	0.27	$\beta<0.3$	1120	<335	303	[10]
PMMA	0.37	$0.3<\beta<0.456$	870	260–400	323	[11]
PS	0.46	$0.456<\beta<0.6$	580	265–350	268	[7]
PMnAA [a]						
n=3	0.35	$\beta\approx0.3$	855	≈255	300	[12]
n=5	0.52	$0.3<\beta<0.456$	520	160–240	272	[12]
n=8	0.58	$0.3<\beta<0.456$	390	115–180	227	[12]
PDPT [b]	0.26	$\beta\ll0.3$	1095	≪330	285	[13]
PETP [c]	0.46	$\beta\approx0.456$	1045	≈475	480	[13]
PPTP [d]	0.57	$\beta\approx0.6$	880	≈530	502	[13]
PPIP [e]	0.61	$\beta\approx0.6$	650	≈390	395	[13]
Epoxy resin						
100%	0.42	$0.456<\beta<0.6$	1100	500–660	462	[14]
70%	0.41	$0.3<\beta<0.456$	615	185–280	252	[15]
+RD [f]	0.37	$\beta\approx0.3$	830	≈250	307	[16]
AgI–Ag_2MoO_4						
40% AgI	0.50	≥0.6 [g]	640	≥380	320	[17]
50% AgI	0.55	≤0.6 [g]	505	≤300	278	[17]
60% AgI	0.65	$\gg0.6$ [g]	360	≫215	233	[17]
AgI–$AgPO_3$–Ag_2MoO_4						
0/75/25	0.68	0.6 [h]	505	>300	345	[18]
30/52/18	0.68	≈0.6 [h]	405	≈240	277	[18]
50/38/12	0.68	$0.456<\beta<0.6$ [h]	450	205–270	305	[18]

[a] Polymethyl (α-*n*-alkyl) acrylates.
[b] Polydipropylene terephthalate.
[c] Polyethylene terephthalate.
[d] Polypropylene terephthalate.
[e] Polypropylene isophthalate.
[f] Reactive diluent.
[g] Estimated from unpublished data obtained on glasses described in reference 17.
[h] Estimated from unpublished data obtained on glasses described in reference 18.

between the curve-fitting and peak-shift methods in some quantitative evaluations of the parameters, the phenomenological models have had a remarkable success in describing qualitatively the response of glasses to a rather wide range of thermal histories. These responses may include a number of apparently strange features, which may be illustrated by the following examples. Cooling and then reheating a glass without any annealing gives rise to an endothermic peak whose magnitude decreases with the increasing ratio of cooling rate to heating rate [19]. A rapidly quenched glass can give rise to double peaks in the heating scan, with the 'sub-T_g' peak increasing in magnitude and temperature as the annealing time below T_g is increased, whereas the 'upper' peak remains invariant [20]. More complex thermal histories can result in an isothermal relaxation in which the response is initially to depart further from equilibrium before returning to the expected approach towards equilibrium [21]. All of these behaviours are predicted by these phenomenological models. If there is a lack of quantitative agreement, and

alternative models are proposed to overcome this, then the new models must also be capable of describing these qualitative features.

A comparison of the data in Table 1 with the corresponding values in Ref. [5] for polyvinyl chloride (PVC), polymethyl methacrylate (PMMA) and polystyrene (PS) shows that the curve-fitting values for x are often smaller than those found by the peak-shift method. A possible explanation for this could lie in the effect of heat transfer and thermal lag, which tends to broaden the DSC response. A broader response is characterised by a wider distribution of relaxation times, and hence by a smaller value of β, which is usually (as discussed below) correlated with smaller values of x.

Hodge [5] was the first to note the rather commonly (but not always) observed correlations between the parameters: small x, small β, large Δh^*. Such correlations can be seen in Table 1 for PVC, PMMA, PS, the alkyl acrylates and the polyesters, as well as for the silver iodomolybdates, though not for the cross-linked epoxy resins. Because of these correlations, the variations in $\beta\Delta h^*$ and $x\Delta h^*$, also given in Table 1, show rather smaller variations than does Δh^* itself.

The interpretation of the physical significance of the parameter values is more controversial, but certain comments can usefully be made. The very large values of apparent activation energy, Δh^*, reflect what is inherent in the term 'apparent', which should preferably always be used in this context. This is an apparent activation energy, because it does not measure the barrier height of the fundamental molecular process, but it measures the effect of the co-operative movement of multiple molecular segments. This co-operativity is an essential feature of the glass-transition phenomena, and is also reflected in the value of β: the smaller is β, the more co-operative is the process. In fact, the coupling model [22] describes the product $\beta\Delta h^*$ as the fundamental activation energy, values of which are listed in Table 1.

The non-linearity parameter x has sometimes been associated with the 'fragility' of glass-forming liquids [23]. Fragile liquids are those with a highly non-Arrhenius temperature dependence, and hence a large apparent activation energy at T_g (hence the correlation between low x and high Δh^*). The glassy-state (constant fictive temperature) apparent activation energy is $x\Delta h^*$ (see Eq. (2)), and the inverse correlation between x and Δh^* implies that the product $x\Delta h^*$ remains relatively constant. This can be seen in Table 1, and means that the glassy-state activation energies are rather constant for a very wide range of different glass-forming systems. The parameter x can, therefore, be considered as a measure of the 'continuity' of behaviour from the melt into the glass [17].

3. Temperature-modulated DSC

The idea of temperature-modulated DSC was first conceived by Reading [24], and was subsequently commercialised by TA Instruments as Modulated DSC (MDSC). A number of variants are now also available, including Alternating DSC (ADSC from Mettler–Toledo) and Dynamic DSC (DDSC from Perkin–Elmer). The basic principle is to superimpose upon the constant heating (or cooling) rate of conventional DSC a periodic modulation of the temperature. The periodic waveform may be of any type, but for convenience is usually sinusoidal. The temperature programme may, in this case, be written as:

$$T = T_0 + q_{av}t + A_T \sin(\omega t) \quad (4)$$

where T_0 is an initial temperature for the modulated scan, q_{av} the average or underlying heating rate, A_T the amplitude of temperature modulations, and ω the angular frequency of the modulations (alternatively, one may write the period of the modulations as per$=2\pi/\omega$). The time derivative of Eq. (4) gives the heating rate modulations:

$$q = q_{av} + A_T\omega\cos(\omega t) \quad (5)$$

which can be seen to be completely defined by the three experimental parameters q_{av}, A_T and ω (or per).

The analysis of the data from temperature-modulated DSC requires a Fourier transformation of the modulated heating rate and heat-flow signals, which is usually done over a sliding single cycle of the heating rate. This transformation yields average values ($\langle q\rangle$ and $\langle \mathrm{HF}\rangle$) and amplitudes ($A_q$ and A_{HF}) for both the heating rate and heat-flow signals, respectively, as well as a phase angle (ϕ) between the heating rate and heat flow. From these transformed quantities, average and complex specific heat capacities may

be defined, respectively, as follows [25]:

$$\langle C_p \rangle = \langle HF \rangle / \langle q \rangle \quad (6)$$

$$C_p^* = A_{HF}/A_q \quad (7)$$

The complex specific heat capacity may be separated into real (in-phase) and imaginary (out-of-phase) parts, respectively, using the phase angle:

$$C_p' = C_p^* \cos\phi \quad (8)$$

$$C_p'' = C_p^* \sin\phi \quad (9)$$

The response of polymer glasses to temperature-modulated DSC in the transition region is now quite well established experimentally (see, e.g. Refs. [26,27]), and essentially consists of the following three important features:

(i) the average specific heat capacity is very similar to that obtained by conventional DSC at the average heating rate, and includes, in particular, the endothermic peak due to relaxation;
(ii) the complex specific heat capacity exhibits a simple sigmoidal change from a glassy value to a liquid-like value over a certain temperature interval, the mid-point temperature of which (T_{mid}) increases with decreasing period of modulation; and
(iii) the negative phase angle (phase angles are usually negative in the glass-transition region as the heat flow lags behind the heating rate) passes through a peak, with a maximum of the order of up to a few tenths of a radian, as the glass-transition interval is traversed.

An illustration of these features is given in Fig. 5 for the glass-transition region of a fully cured epoxy resin [28]. It should be noted that the average heat capacity in item (i) is proportional to the heat-flow signal in Fig. 5, which shows only a very small endothermic peak as the thermal cycle involved no annealing prior to the temperature-modulated scan. All of these features may be described qualitatively using the TNM model with a single relaxation time [29–31], with some typical model predictions shown in Fig. 6; a quantitative analysis is currently in progress using the TNM model with a distribution of relaxation times. Thus, there is clearly scope for an interpretation of the response of polymer glasses to temperature-modulated DSC in the context of existing models for

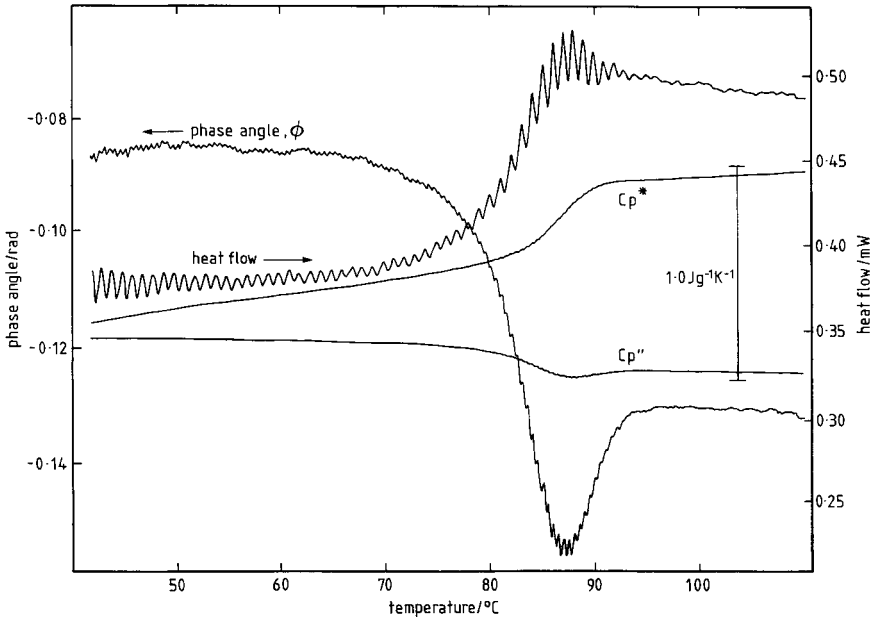

Fig. 5. Alternating DSC scan (Mettler–Toledo STAR^e system) through the glass-transition region of a fully cured epoxy resin of sample mass 20.15 mg using the following conditions: q_{av}=1°C/min; A_T=1°C; and per=1 min [28].

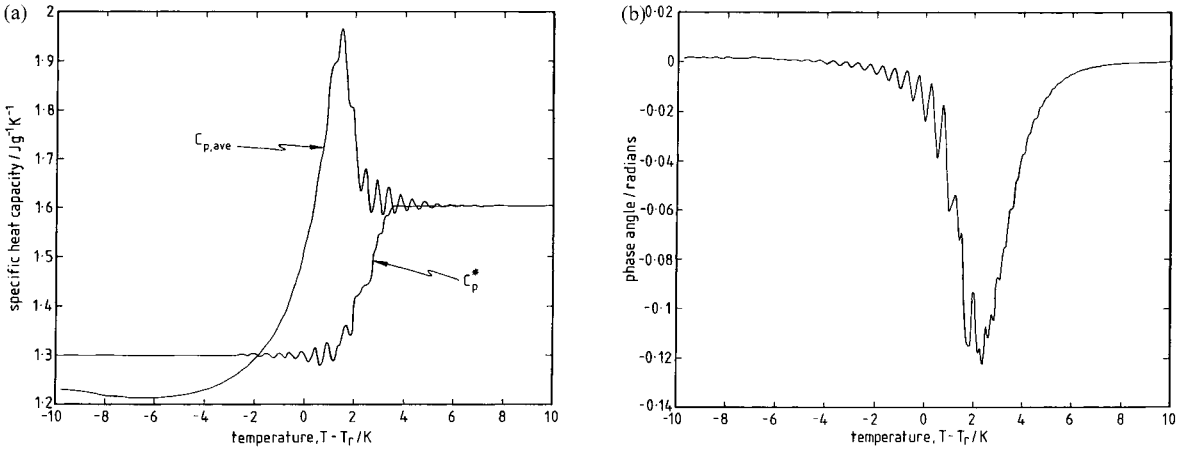

Fig. 6. Predictions of single parameter TNM model for (a) average specific heat capacity and complex specific heat capacity, and (b) phase angle for an amorphous polymer in the glass-transition region. The experimental conditions are: q_{av}=0.5°C/min; A_T=0.25°C; and per=1 min.

relaxation behaviour, and some current ideas may be summarised as follows.

3.1. Average specific heat capacity

This is essentially equal to the specific heat capacity that would be obtained by conventional DSC at the underlying heating rate. However, the extent to which this is observed in practice is rather difficult to establish, as the quality of the average signal from TMDSC requires to be improved by smoothing, while the quality of the conventional DSC signal is not particularly good at the typical underlying heating rates of TMDSC (for example 1 K/min). Thus, there would be no advantage to be gained by studying enthalpy relaxation, for example, by means of $\langle C_p \rangle$ from TMDSC instead of by conventional DSC.

3.2. Complex specific heat capacity

The 'step change' in C_p^* from a glassy to a liquid-like value at a temperature denoted by T_{mid} occurs for the following reason. In the glassy region, the average molecular relaxation time, $\langle \tau_{mol} \rangle$, is much longer than the period, per, of the imposed modulations; hence, during any one period, the glass has not sufficient time for the structure to follow the temperature changes, and the response will be 'thermally elastic'. As a consequence, the value of C_p^* will be a glassy value, and the phase angle will be zero. In contrast, in the liquid-like region, $\langle \tau_{mol} \rangle$ will be much shorter than per, and the structure can follow all the imposed temperature modulations, with the result that the response is liquid-like. Here, the value of C_p^* will be that of the liquid, while the phase angle will once again be zero. In the transition interval, the response will be critically dependent on the magnitude of $\langle \tau_{mol} \rangle$, which decreases as the average temperature increases, and the mid-point of the transition will occur approximately when $\langle \tau_{mol} \rangle \approx$per; hence, T_{mid} increases as the modulation period decreases. This dependence has been observed experimentally, and is shown in Fig. 7 for a polycarbonate sample. It is possible from such data to evaluate the apparent activation energy, or the parameter θ (refer to Eq. (1)), from [29–31]:

$$\mathrm{d}\ln(\mathrm{per})/\mathrm{d}T = -\theta \tag{10}$$

Although this may appear an attractive alternative to the usual 'fictive temperature method' for the determination of the apparent activation energy [3], it suffers from the drawback that only a limited interval of the period is available in practice, at best a decade, whereas the fictive temperature method can provide at least four decades of cooling rate quite easily. Indeed, this drawback is well illustrated by the results in Fig. 7, for which a range of only one decade in the period could be used, and for which the stray data

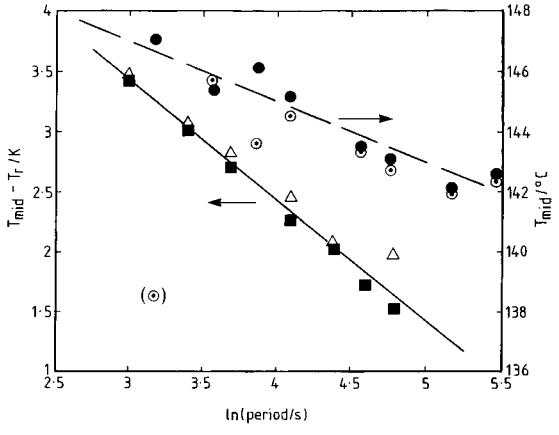

Fig. 7. Theoretical dependence of T_{mid} on ln (period) for (■) cooling, and (Δ) heating, when θ=1.0 K^{-1} (full line), and experimental data for polycarbonate for (○) A_T=0.5 K and (●) 1.0 K, from which θ=0.5 K^{-1} ($\Delta h^* \approx$720 kJ/mol).

point at the shortest period (24 s) indicates an inability of the sample to follow the rather rapidly changing temperature modulations.

It may also be of some interest to analyse the width of the transition in C_p^*, as it is supposedly uncomplicated by any annealing or relaxation effects. At present, however, no useful theoretical predictions are available which can separate the effects of non-linearity (x) from those of non-exponentiality (β) in this respect. One would clearly anticipate a broadening of this transition as β decreases, but the interaction of this with the influence of x would need to be established before this feature could be used as a means of evaluating the non-exponentiality parameter.

In fact, although it is usually assumed that C_p^* is rather unaffected by annealing, this is only an approximation. Increased annealing has been observed experimentally to sharpen this transition, and this effect is also predicted by the theoretical model. Hence, further care would need to be exercised in the interpretation of the width of this transition in terms of non-exponentiality.

3.3. Phase angle

The maximum in the negative phase angle in the transition region occurs for the same reason as for the step change in the complex specific heat capacity. Likewise, the breadth of the transition could be analysed in terms of the peak width at half height, for example, but subject again to the same reservations as for C_p^*; namely, the interaction between x and β, and the sharpening of the peak with increased annealing. In addition, however, the quantitative analysis of the phase angle is complicated by heat-transfer effects, similar to those discussed above in respect of the curve-fitting method of evaluation in conventional DSC. Hence, an appropriate correction procedure must be adopted, such as that suggested by Schick et al. [32], and outlined below.

It is argued above that the phase angle should be zero in the glassy and liquid-like regions. In practice, this is rarely observed in the uncorrected data, and can clearly be seen from Fig. 5. The reason is that an 'instrumental' phase angle is introduced because of the non-ideal heat transfer between instrument and sample, and this is additional to any phase angle resulting from relaxation effects in the polymer glass. The instrumental phase angle depends on the experimental TMDSC parameters, and to a first approximation may be expressed as follows [26]:

$$\phi = \arctan\left(mC_p^*\omega/K\right) \tag{11}$$

where m is the mass of the sample and K an instrumental parameter describing the heat-transfer characteristics of the system. This dependence of the phase angle on sample mass and modulation frequency, and its independence of the amplitude of the modulations, has been investigated experimentally [33]. Furthermore, its dependence on C_p^* is clearly evident from the different non-zero values of ϕ before and after the transition, and this observation justifies the following correction procedure [32,33].

The instrumental phase angle follows the complex specific heat capacity according to Eq. (11). For small phase angles, which is usually the case in the glass-transition region of polymers, this implies a linear relationship between instrumental phase angle and C_p^* for fixed values of m, ω and K. Accordingly, by scaling C_p^* such that it matches the measured phase angle in the glassy and liquid-like regions, a baseline for the instrumental phase angle is constructed. Subtracting this instrumental baseline will yield the corrected phase angle, which will be zero both before and after the transition as anticipated, and which will now reflect only the phase angle changes due to structural relaxation effects in the sample. Once this phase angle

correction has been made, it is then possible to calculate the in-phase and out-of-phase components of C_p^* defined by Eqs. (8) and (9).

3.4. In-phase specific heat capacity

As the phase angle in the glass-transition region is usually small, and hence cos ϕ is rather close to unity, the complex and in-phase specific heat capacities are almost indistinguishable. No further significant information is, therefore, available from C_p' than is already available from C_p^*.

3.5. Out-of-phase specific heat capacity

Similarly, because the phase angle is small, C_p'' is very similar to the phase angle itself ($\sin\phi \approx \phi$), though modified slightly by the changing value of C_p^* through the transition region. For example, C_p'' displays a peak at essentially the same temperature as does ϕ, and is zero before and after the transition. The area under the C_p'' peak has been the subject of some discussion, but it is clear that it does not measure the amount of enthalpy that may have been lost during a prior annealing process; the theoretical model [31] predicts an invariant peak area as the annealing time increases. There may, on the other hand, be some insight to be gained from an interpretation of this area in terms of entropy changes taking place within the sample during any one period of the modulations, which could be discussed more appropriately within the context of the Adam–Gibbs configurational entropy model [34] rather than the TNM model for structural relaxation.

4. Conclusions

The Tool–Narayanaswamy–Moynihan model for structural relaxation in polymer (or other) glasses in the transition region is remarkably successful in describing the characteristic features observed experimentally by DSC following even rather complex thermal histories. Nevertheless, discrepancies between parameter values reported by different authors and for different experimental conditions clearly exist, and their interpretation must therefore be undertaken with some care. However, a careful consideration of the experimental conditions under which they have been evaluated, and a critical appraisal of the evaluation procedures used, should help in eliminating some of the discrepancies.

The model is equally successful in describing the characteristic features of the response of glasses to the new technique of temperature-modulated DSC. In addition, this technique may provide scope for further insight, for example through an analysis of the out-of-phase component of the complex specific heat capacity. Again, however, quantitative evaluation should be undertaken with some care, particularly in the light of problems introduced by heat transfer effects.

Acknowledgements

The author wishes to acknowledge his colleagues Corrie Imrie and Zhong Jiang, as well as the financial support of Mettler–Toledo GmbH, in respect of the temperature modulated DSC work reported here. He also acknowledges the permission of Salvador Montserrat to reproduce his unpublished data on epoxy resin.

References

[1] O.S. Narayanaswamy, J. Am. Ceram. Soc. 54 (1971) 491.
[2] A.Q. Tool, J. Am. Ceram. Soc. 29 (1946) 240.
[3] C.T. Moynihan, A.J. Easteal, M.A. DeBolt, J. Tucker, J. Am. Ceram. Soc. 59 (1976) 12.
[4] A.J. Kovacs, J.J. Aklonis, J.M. Hutchinson, A.R. Ramos, J. Polym. Sci., Polym. Phys. Edn. 17 (1979) 1079.
[5] I.M. Hodge, J. Non-Cryst. Solids 169 (1994) 211.
[6] J.M. O'Reilly, CRC Critical Rev. Sol. Stat. Mater. Sci. 13(3) (1987) 259.
[7] J.M. Hutchinson, M. Ruddy, J. Polym. Sci., Polym. Phys. Edn. 26 (1988) 2341.
[8] J.M. Hutchinson, Progr. Coll. Polym. Sci. 87 (1992) 69.
[9] J.M. Hutchinson, Polymer International 47 (1998) 56.
[10] A.J. Pappin, J.M. Hutchinson, M.D. Ingram, Macromolecules 25 (1992) 1084.
[11] J.M. Hutchinson, M.D. Ingram, A.J. Pappin, unpublished data.
[12] M.-E. Godard, J.-M. Saiter, P. Cortés, S. Montserrat, J.M. Hutchinson, F. Burel, C. Bunel, J. Polym. Sci., Polym. Phys. Edn. 36 (1998) 583.
[13] P. Cortés, S. Montserrat, J. Polym. Sci., Polym. Phys. Edn. 36 (1998) 113.
[14] S. Montserrat, P. Cortés, A.J. Pappin, K.H. Quah, J.M. Hutchinson, J. Non-Cryst. Solids 172–174 (1994) 1017.

[15] J.M. Hutchinson, D. McCarthy, S. Montserrat, P. Cortés, J. Polym. Sci., Polym. Phys. Edn. 34 (1996) 229.
[16] P. Cortés, S. Montserrat, J.M. Hutchinson, J. Appl. Polym. Sci. 63 (1997) 17.
[17] M.D. Ingram, J.M. Hutchinson, A.J. Pappin, Phys. Chem. Glasses 32 (1991) 121.
[18] J.M. Hutchinson, M.D. Ingram, A.J. Pappin, J. Non-Cryst. Solids 131–133 (1991) 483.
[19] J.M. Hutchinson, M. Ruddy, J. Polym. Sci., Polym. Phys. Edn. 28 (1990) 2127.
[20] M. Ruddy, J.M. Hutchinson, Polym. Commun. 29 (1988) 132.
[21] A.J. Kovacs, Fortschr. Hochpolym. Forsch. 3 (1963) 394.
[22] K.L. Ngai, Comments on Solid State Physics, 9 (1979) 127; 9 (1980) 141.
[23] C.A. Angell, in K.L. Ngai, G.B. Wright (Eds.), Relaxations in Complex Systems, 1984, p. 3.
[24] M. Reading, Trends Polym. Sci. 1 (1993) 248.
[25] J.E.K. Schawe, Thermochim. Acta 260 (1995) 1.
[26] B. Wunderlich, Y. Jin, A. Boller, Thermochim. Acta 238 (1994) 277.
[27] A. Hensel, J. Dobbertin, J.E.K. Schawe, A. Boller, C. Schick, J. Therm. Anal. 46 (1996) 935.
[28] S. Montserrat, private communication.
[29] J.M. Hutchinson, S. Montserrat, J. Therm. Anal. 47 (1996) 103.
[30] J.M. Hutchinson, S. Montserrat, Thermochim. Acta 286 (1996) 263.
[31] J.M. Hutchinson, S. Montserrat, Thermochim. Acta, 304/305 (1997) 257.
[32] S. Weyer, A. Hensel, C. Schick, Thermochim. Acta, 304/305 (1997) 267.
[33] Z. Jiang, C.T. Imrie, J.M. Hutchinson, Thermochim. Acta, 315 (1998) 1.
[34] G. Adam, H.J. Gibbs, J. Chem. Phys. 43 (1965) 139.